doi: 10.56761/EFRE2022.C3-O-024201

Optical absorption of radiation defects in alkali halide crystals implanted magnesium and silver ions

V. Paperny[1,], N. Ivanov[2], S. Nebogin[2], L. Bryukvina[3]*

[1]*Irkutsk State University, Irkutsk, Russian Federation*
[2]*Irkutsk National Research Technical University, Irkutsk, Russian Federation*
[3] *Irkutsk Branch of Institute of Laser Physics SB RAS, Irkutsk, Russian Federation*
[*]*paperny@yandex.ru*

Abstract. The results of a research of the properties, structure, and formation mechanisms of metallic magnesium and silver nanoparticles obtained by ion implantation in LiF, NaCl, KCl, and KBr crystals. The crystal samples were irradiated with accelerated Mg^+ ions, with the mean energy of ~80 keV, the mean ion current density of ~4 μA/cm^2 produced with a small-sized ion implanter. Dose ranges from $2.2 \cdot 10^{16}$ to $7.5 \cdot 10^{16}$ ion/cm^2. Comparison of the optical properties of crystals implanted with magnesium and silver ions shows a significant superiority of the optical characteristics in the case of implantation with magnesium ions.
Keywords: ion implantation, alkali halide crystals, optical absorption, magnesium, silver.

1. Introduction

Crystal structures with metal nanoparticles have properties that allow them to be used in one of the main branches of nanotechnology – nanoplasmonics. The physical phenomena observed in nanoplasmonics arise in metallic nanoparticles when they interact with an external electromagnetic radiation and with various atomic and molecular structures. Nanoparticles smaller of the light wavelength can originate light-induced collective electronic oscillations known as local surface plasmon resonance (LSPR) [1]. The resonant wavelength in LSPR is sensitive to the environment, which is the basis for a number of sensor applications [2, 3]. The unique properties of metallic nanoparticles led to the manifestation of a number of new effects, such as: giant Raman scattering of light (SERS) [4], an increase in the absorption cross section and fluorescence quantum yield of various molecules when exposed to a local enhanced field in the vicinity of nanoparticles [5, 6]. Such metals as Ag, Au, Al, which are widely used for these purposes, are characterized by minimal dissipative losses in the UV and visible regions of the spectrum. A feature of the optical properties of these metals is the presence of a wide range of wavelengths in which the excitation of surface plasmons is possible. However, Ag and Au are rare and expensive; in addition, Ag undergoes oxidation, which significantly affects its optical properties.

Of the various plasmonic materials studied, Mg has attracted particular attention because it can support localized surface plasmon resonance with a high extinction value in the UV range. Magnesium also provides significantly higher absorption efficiency in the far zone and a significant increase in the electric field in the near zone [7].

The aim of this work was to study the optical properties, including the enhancement of the luminescence of color centers in a wide range of alkali halide single crystals (AHCs) (LiF, NaCl, KCl and KBr) implanted with Mg and Ag ions. Such crystals, especially LiF, are used in laser physics and dosimetry [8, 9] and in the physics of fundamental phenomena [10–13]. These applications are based on the luminescence of color centers formed in crystals due to radiation exposure, incl. due to ion implantation. Previously, we have shown that Mg ion implantation significantly increases the luminescence intensity of F_3 like color centers in LiF crystals [6]. Ion implantation, in contrast to irradiation with X-rays, γ-radiations, electrons, neutrons, can radically change the composition of color centers, the intensity of their absorption and luminescence.

To achieve the goal of the work, it was necessary to find out, on the one hand, whether there is a commonality in the properties of various AHCs when implanted with Mg and Ag metal

nanoparticles, and on the other hand, what is the difference in the efficiency of affecting the optical properties of crystals of two different types of metal nanoparticles.

2. Experimentals

Crystals of LiF, NaCl, KCl, and KBr were grown by the Kyropoulos method from melts of the corresponding salts. Then the crystals were irradiated by means of original pulsed compact source of accelerated ions with Mg and Ag ions with an average energy of ~80 keV and an average current density in the ion beam of 4 μA/cm^2. Irradiation doses were in the range from $2.2 \cdot 10^{16}$ to $7.5 \cdot 10^{16}$ ion/cm^2. Nanoparticles and color centers were formed in a thin near surface layer on the order of 60–100 nm.

In order to control the absence of extraneous impurity ions in crystals, the content of magnesium and hydroxyl ions in crystals was estimated from the IR spectra of "free" and "perturbed" by magnesium OH^- ions [14]. IR spectra were measured on a Bruker Vertex 70 Fourier spectrometer. UV and visible absorption spectra were measured on a Shimadzu UV-3600 spectrometer. The spectra were measured at room temperature. The luminescence spectra of the samples were studied using a Shimadzu RF-5301PC spectrofluorimeter.

3. Results and discussion

3.1. Mg implanted AHCs

The absorption spectra of magnesium-implanted samples are shown in Fig.1. The figure shows that due to the implantation of KCl, KBr and NaCl crystals by magnesium ions, an absorption band with λ_{max} = 320 nm was formed. In LiF crystals, an absorption band λ_{max} = 264 nm is observed. The centers responsible for the 320 nm band in NaCl and KBr crystals turned out to be unstable. The absorption band with λ_{max} = 320 nm decreased by near 2 times in NaCl and 3.5 times in KBr after several hours of storage at room temperature. In KCl, the absorption band is also annealed at temperatures up to 300 °C. Temperature dependences of the intensity of the absorption band after implantation, for example, are shown in Fig.2a and Fig.2b for LiF crystals at λ_{max} = 264 nm and for NaCl crystal at λ_{max} = 320 nm.

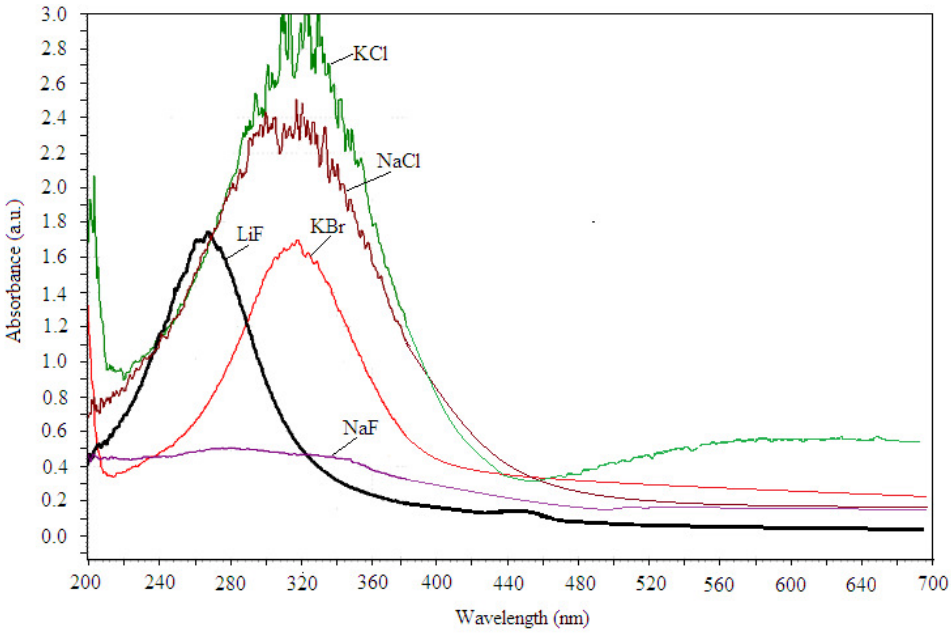

Fig.1. Absorption spectra of LiF, KCl, NaCl, KBr and NaF crystals after Mg-ions implantation. T_{meas} = 300 K.

In addition, short-term irradiation of all the implanted crystals under study with X-rays leads to a decrease in the intensity of only the 320-nm band in KCl, NaCl, and KBr, while the 264-nm band in LiF almost not changes after irradiation. On Fig.3a and Fig.3b shows the absorption spectra of the implanted KCl and NaCl crystals before and after exposure to X-rays for 2 min, demonstrating this behavior of the absorption bands. A significant decrease in the intensity of the bands at 320 nm and the appearance of a band of F centers (at 470 nm for NaCl and 560 nm for KCl) are observed, which indicates the F-like nature of the centers responsible for the 320 nm band, while the behavior of the 264 nm band in LiF is characteristic of LSPR.

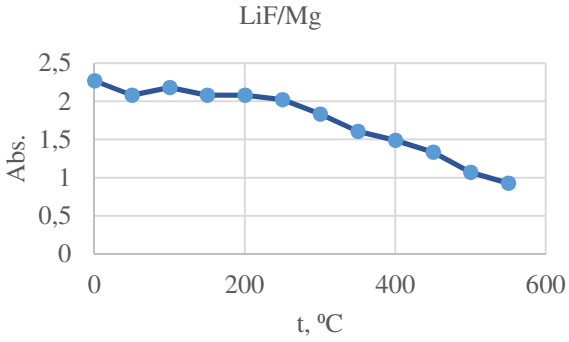

Fig.2a. Temperature dependence of absorption at λ_{max} = 264 nm in LiF crystal implanted Mg ions.

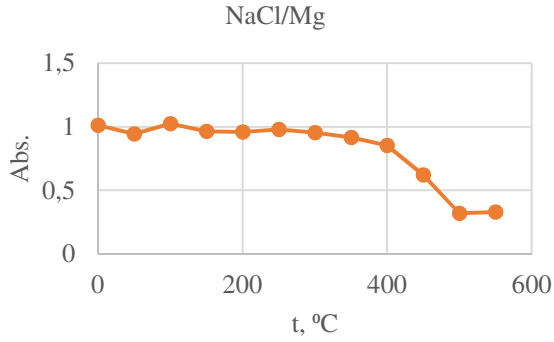

Fig.2b. Temperature dependence of absorption at λ_{max} = 320 nm in NaCl crystal implanted Mg ions.

The band with λ_{max} = 320 nm is uniquely associated with magnesium. However, the centers responsible for this band are stable only in the LiF crystal up to a temperature of 600 °C. It can be assumed that plasmon resonance band of Mg nanoparticles with λ_{max} = 264 nm is observed in LiF. The position of the plasmon resonance band of Mg nanoparticles can be calculated using the Mie theory for the absorption of light by metal spheres [15].

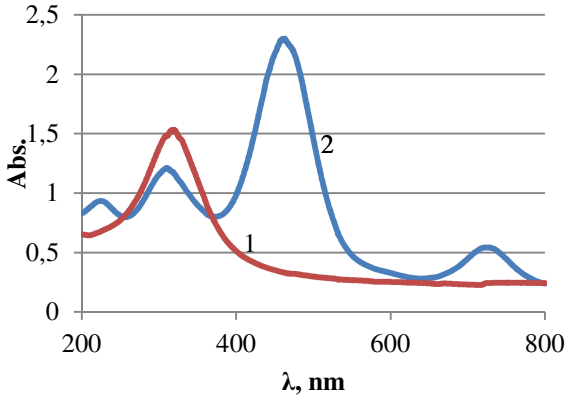

Fig.3a. Absorption spectra of NaCl crystal implanted Mg ions before (1) and after (2) X-ray irradiation during 2 min, 60 kV, 50 mA.

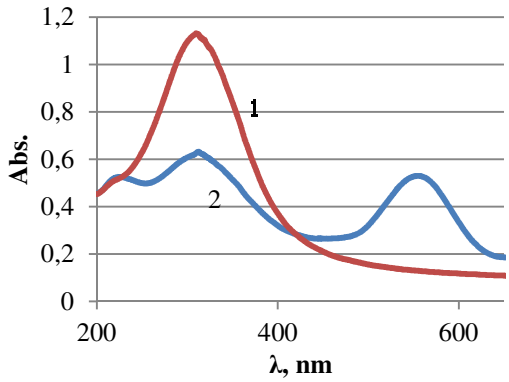

Fig.3b. Absorption spectra of KCl crystal implanted Mg ions before (1) and after (2) X-ray irradiation during 2 min, 60 kV, 50 mA.

It is known that the wavelength of maximum absorption in the band can be calculated by the formula $\lambda_0 = (1 + 2n_0^2)^{1/2}\lambda_c$, here n_0 is the refraction index of the host medium, λ_c is the Wood-Zener wavelength for the onset of ultra-violet transparency of the metal. This relation holds for spherical particles which are small compared with the wavelength λ_0 [15]. The wavelengths of the Mg

plasmon band maxima calculated using this formula is presented in Table 1 in comparison with the experimental data. The refractive index of AHCs at a wavelength of 280.4 nm is taken from [16], the value λ_c = 117 nm for Mg is from [17].

Table 1. Maximum values of plasmon resonance bands Mg nanostructures in AHCs

Crystal	Index of refrection	λ_0, nm (calculated)	λ_0, nm (experim.)
LiF	1.4120	262	264
KCl	1.5589	283	320
KBr	1.6714	300	317
NaCl	1.6215	293	317

It follows from Table 1 that the calculated and experimental data for the LiF crystal are close. Considering this, as well as the temperature stability of the absorption band of the crystal with λ_{max} = 264 nm after implantation, we can conclude that it characterizes magnesium nanoparticles. Magnesium nanoparticles in radiation-treated LiF crystals are mentioned in a number of works [18, 19]. Our results agree with them, except that the absorption band of magnesium nanoparticles in these works is in the range of 277–280 nm. The formation of Mg nanoparticles 20–25 nm in size in LiF is also indicated by their presence in the SEM image shown in Fig.4.

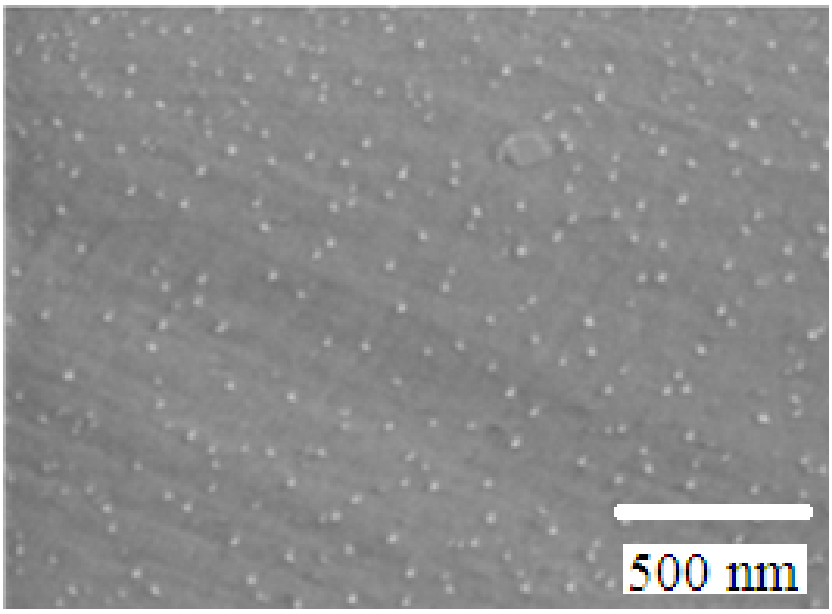

Fig.4. SEM image of the Mg nanoparticles in LiF crystal implanted Mg ions.

To obtain a magnesium atom, from which nanoparticles are then formed, 2 electrons are required. Taking into account the intense formation of nanoparticles during implantation, it can be said that electrons are predominantly involved in the formation of nanoparticles, rather than electron color centers and native colloids of lithium. In this process, anion vacancies are released, to which cation vacancies from impurity-vacancy dipoles are attached. Thus, the necessary space is formed for placing the Mg nanoparticles in LiF.

3.2. Ag implanted AHCs

Implantation of a set of crystals with silver ions also caused the appearance of LSPR bands with maxima in the wavelength range characteristic of Ag nanoparticles (Fig.5).

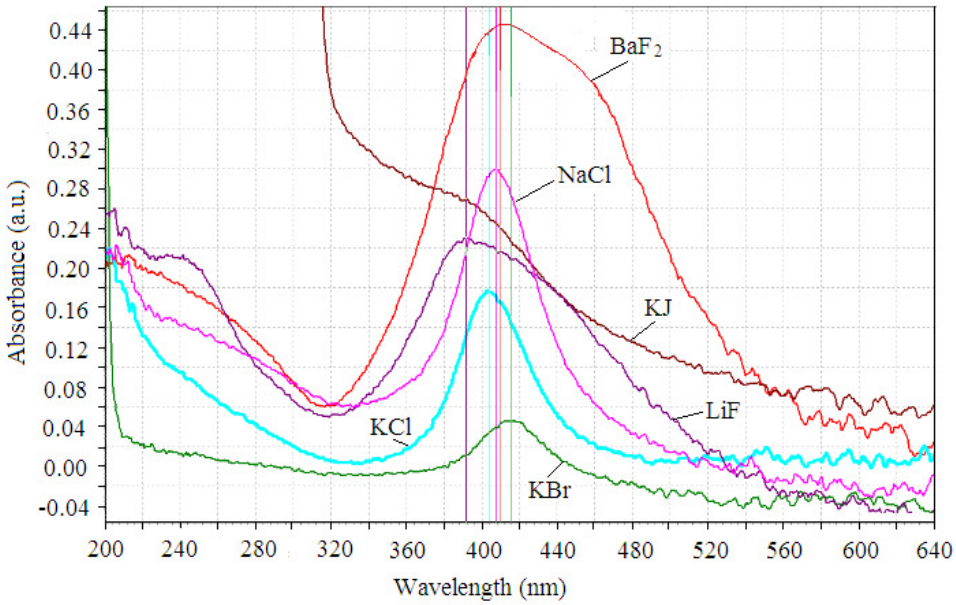

Fig.5. Absorption spectra of LiF, KCl, NaCl, KBr, KJ and BaF_2 after Ag ions implantation.

Similar bands due to the implantation of silver ions were observed in [20]. The wavelengths of the maxima of the LSPR bands of Ag nanoparticles in the matrices studied by us are given in Table 2.

Table 2. Wavelength of absorption bands maximum in AHCs after Ag ions implantation

Crystal type	λ_{max}, nm
LiF	392
KCl	404
NaCl	408
KBr	415
KJ	–
BaF_2	410

4. Conclusion

The implantation of alkali halide crystals with metal ions leads to a significant change in the optical characteristics associated both with the formation of radiation defects, which include metal ions in their composition, and with the formation of metal nanoparticles, as is observed in implanted LiF crystals with Mg ions. Note that radiation defects created by implantation have extremely high absorption coefficients in a thin layer of the implanted area. So for KCl and NaCl in the region of about 100 nm, the absorption coefficient reaches 10^6–10^7 cm^{-1}.

What defects are formed in the process of implantation, in all likelihood, depends significantly on the ratio of the ionic radii of the implanted metals and the lattice constant of the crystal. Thus, for a LiF crystal with a lattice constant of 4.03 Å, the ionic radius of Mg (0.72 Å) is close in size to the ionic radius of lithium (0.74 Å) and the diffusion of ions and atoms is difficult, which leads to the formation of metal nanoparticles in the local region of the lattice when the critical concentration of Mg atoms is reached. The lattice constant of KCl, NaCl, and KBr crystals is much larger, which promotes effective thermal diffusion of Mg atoms and ions in these crystals, with the formation of F-like defects distributed over the lattice, responsible for the absorption band at 320 nm. This assumption is also confirmed by the results on the implantation of silver ions into AHCs, where nanoparticles are formed (plasmon resonance at about 400 nm) due to the significantly larger ionic radius of Ag compared to Mg.

Acknowledgement

This work was supported by Ministry of Science and Higher Education of the Russian Federation in the framework of the scientific and educational center “Baikal” (grant no. FZZS-2021-0007) and RFBR (grant no. 20-02-00322).

5. References

[1] Willets K.A., Van Duyne R.P., *Annu. Rev. Phys. Chem.*, **58**, 267, 2007; doi: 10.1146/annurev.physchem.58.032806.104607
[2] Yao J.M., Le A.-P., Gray S.K., Moore, J.S., Rogers, J.A., Nuzzo, R.G., *Adv. Mater.*, **22**, 1102, 2010; doi: 10.1002/adma.200904097
[3] Mayer K.M., Hafner J.H., *Chem. Rev.,* **111**, 3828, 2011; doi: 10.1021/cr100313v
[4] Sharma Bhavya, Frontiera Renee R., Henry Anne-Isabelle, Ringe Emilie and Van Duyne Richard P., *Materialstoday*, **15**(1–2), 16, 2012; doi: 10.1016/S1369-7021(12)70017-2
[5] De Melo L.S.A., Chaves C.R., Filho P.E.C., Saska S., Nigoghossian K., Gomes A.S.L., Messaddeq Y., Ribeiro S.J.L., Santos B.S., Fontes A., R.E. de Araujo, *Plasmonics*, **8**, 1147, 2013; doi: 10.1007/s11468-013-9524-z
[6] Nebogin S.A., Ivanov N.A., Bryukvina L.I., Shipitsin N.V., Rzhechitskii A.E., Papernyi V.L., *PNFA* **29**, 36, 2018; doi: 10.1016/j.photonics.2018.01.005
[7] Sanz J. M., Ortiz D., Alcaraz de la Osa R., Saiz J. M., Gonzaĺez F., Brown A. S., Losurdo M., Everitt H. O. and Moreno F., *J. Phys. Chem. C*, **117**, 19606, 2013; doi: 10.1021/jp405773p
[8] Basiev T.T., Bykovsky N.E., Konyushkin V.A., Senatsky Yu.V., *Quantum Electronics*, **34**(12), 1138, 2004; doi: 10.1070/QE2004v034n12ABEH002751
[9] Tang K., Zhang S., *Radiation Measurements*, **145**, 106607, 2021; doi: 10.1016/j.radmeas.2021.106607
[10] Ivanov N.A., Paperny V.L., Kolesnikov S.S., Nebogin S.A. and Bryukvina L.I., *Surface. X-Ray, Synchrotron and Neutron Research*, **9**, 1, 2022; doi: 10.31857/S1028096022090059
[11] Ivanov N.A., Nebogin S.A., Kolesnikov S.S., Bryukvina L.I., *Phys. Sol. State*, **63**(9), 1502, 2021; doi: 10.1134/S1063783421090134
[12] Bryukvina L.I., Ivanov N.A., Glazunov D.S., *AIP Conf. Proc.*, **2392**, 020002, 2021; doi: 10.1063/5.0061993
[13] Bryukvina L.I., Glazunov D.S., *AIP Conf. Proc.*, **2392**, 040001, 2021; doi: 10.1063/5.0061996
[14] Stoebe T.G., *J. Phys. Chem. Sol.*, **28**(8), 1375, 1967; doi: 10.1016/0022-3697(67)90266-1
[15] Doyle W. T., *Proc. Phys. Soc.*, **75**, 649, 1960; doi: 10.1088/0370-1328/75/5/303
[16] Li H. H., *J. Phys. Chem. Ref. Data,* **5**, 329, 1976; doi: 10.1063/1.555536
[17] Ringe E., *J. Phys. Chem. C,* **124**(29), 15665, 2020; doi: 10.1021/acs.jpcc.0c03871
[18] Davidson A.T., Camins J.D., Raphuthi A.M.J., Kozakiewicz A.*G.*, Sendezera E.J., Derrys T.E., *J. Phys.: Condens. Matter*, **7,** 3211, 1995; doi: 10.1088/0953-8984/7/17/005
[19] Lushchik A., Lushchik Ch., Schwartz K., Vasil’chenko E., Papaleo R., Sorokin M., Volkov A. E., Neumann R., Trautmann C., *Phys. Rev. B*, **76**, 054114, 2007; doi: 10.1103/PhysRevB.76.054114
[20] Shipilova O.I., Dresvyansky V.P., Martynovich E.F., Rakevich A.L., Shendrik R.Yu., Paperny V.L., Chernich A.A., *IOP Conf. Series: J.of Phys.: Conf. Ser.*, **830**, 012145, 2017; doi: 10.1088/1742-6596/830/1/012145